Biochemistry

 Volume 42, Number 39 October 7, 2003

Articles

RNA−Ligand Interactions: Affinity and Specificity of Aminoglycoside Dimers and Acridine Conjugates to the HIV-1 Rev Response Element†

Nathan W. Luedtke,§ Qi Liu, and Yitzhak Tor*

Department of Chemistry and Biochemistry, University of California, San Diego, La Jolla, California 92093-0358

Received May 9, 2003; Revised Manuscript Received July 28, 2003

ABSTRACT: Semisynthetic aminoglycoside derivatives may provide a means to selectively target viral RNA sites, including the HIV-1 Rev response element (RRE). The design, synthesis, and evaluation of derivatives based upon neomycin B, kanamycin A, and tobramycin conjugates of 9-aminoacridine are presented. To evaluate the importance of the acridine moiety, a series of dimeric aminoglycosides as well as unmodified "monomeric" aminoglycosides have also been evaluated for their nucleic acid affinity and specificity. Fluorescence-based binding assays that use ethidium bromide or Rev peptide displacement are used to quantify the affinities of these compounds to various nucleic acids, including the RRE, tRNA, and duplex DNA. All the modified aminoglycosides exhibit a high affinity for the Rev binding site on the RRE ($K_d \leq 10$ nM), but few compounds have a high specificity for the RRE. Compared to the acridine conjugates, the dimeric and unmodified aminoglycosides exhibit good RNA over DNA selectivity, but show little differentiation between different RNA molecules. Neomycin-based derivatives consistently have the highest RNA and DNA affinities, but the lowest RRE specificity. To optimize these derivatives for RRE specificity, a series of neomycin−acridine conjugates with variable linker lengths were synthesized and evaluated. The neo-acridine conjugate with the shortest linker length has the optimal RRE specificity. Duplex DNA, on the other hand, prefers the acridine conjugate with the longest linker length, and duplex RNA (poly r[A]−r[U]) has the highest affinity for the conjugate with an intermediate linker length. Compared to neomycin B, the derivatives based upon tobramycin and kanamycin A have slightly lower RRE affinities, but better RRE specificities. These results illustrate how the binding affinity and specificity of aminoglycoside intercalator conjugates can be tuned by optimizing the linker length and by changing the identity of the aminoglycoside moiety. These results also indicate that many aminoglycoside-based ligands are capable of high-affinity binding of RNA, but achieving high site specificity remains a challenging objective.

Aminoglycoside antibiotics are highly selective in their preferential binding of RNA over DNA, but exhibit much less discrimination between different RNA molecules. Aminoglycosides bind to a wide range of unrelated RNAs, including simple duplex RNA (*1*), 16S and 18S rRNAs (*2*−*4*), mRNA transcripts (*5*), tRNA (*6*), and a variety of catalytic RNAs (*7*). This general affinity for RNA is related to the ability of aminoglycosides to bind the major groove of duplex RNA through electrostatic interactions mediated by their ammonium groups (*1*, *7*, *8*). Aminoglycosides are selective for A-form over B-form type duplexes and can

† This work was supported by the Universitywide AIDS Research Program (ID01-SD-027) and the National Institutes of Health (AI 47673).

* To whom the correspondence should be addressed. Tel: (858) 534−6401. Fax: (858) 534−5383. E-mail: ytor@ucsd.edu.

§ Present address: Department of Chemistry and Biochemistry, Yale University, New Haven, Connecticut 06520-8107.

10.1021/bi034766y CCC: $25.00
Published on Web 09/12/2003

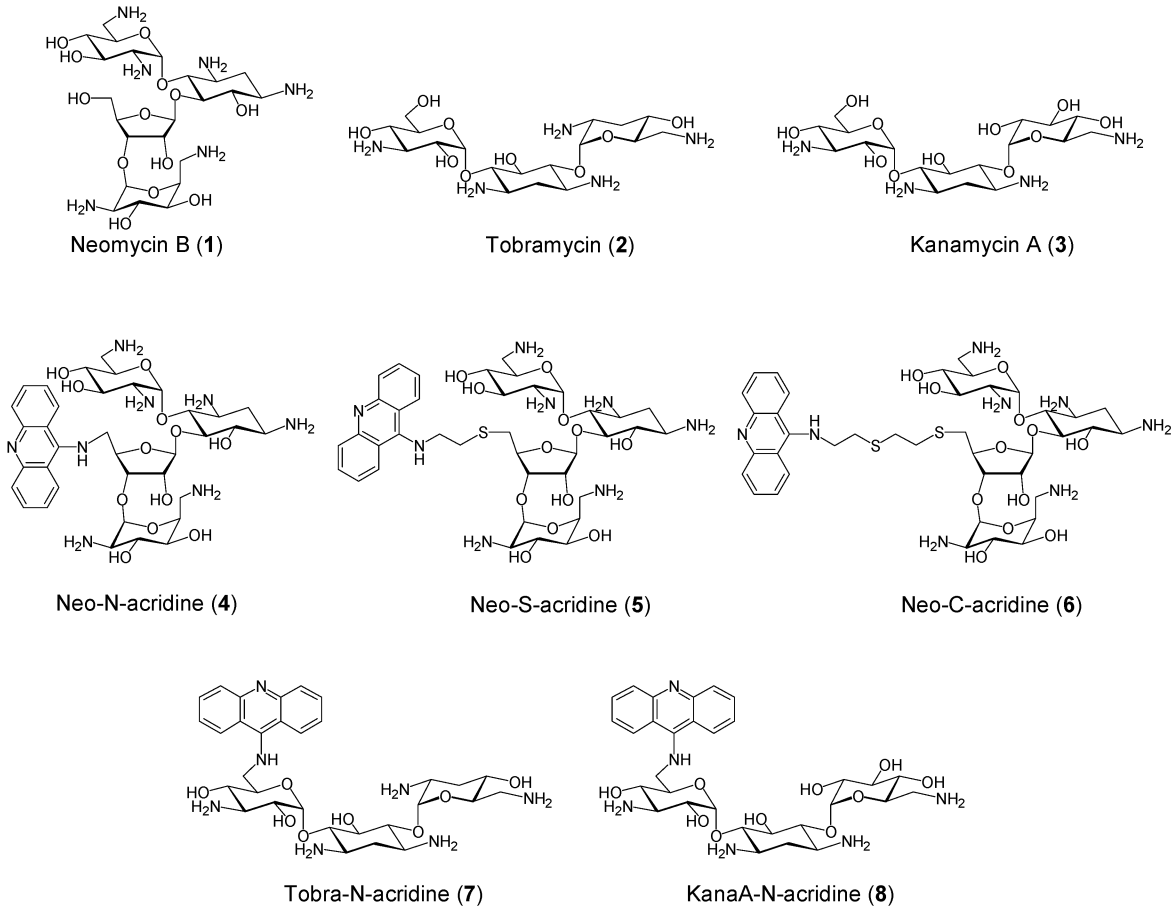

FIGURE 1: Structures of the unmodified aminoglycosides **1**−**3**, and aminoglycoside−acridine conjugates **4**−**8**. The primary hyrdoxyls of the aminoglycosides have been used for acridine conjugation (see Suppporting Information for synthesis and characterization of **4**, **6**, **7**, and **8**). The amines of aminoglycosides can be used for "one step" conjugation reactions with dye molecules (*33*). Amines are, however, known to be essential for RNA binding (*1*). Elimination of hydroxyls, on the other hand, does not necessarily interfere with aminoglycoside−RNA binding (*49*).

facilitate the conformational change of calf thymus (CT)[1] DNA from a B-form into an A-form double helix (*9*, *10*). Many RNA molecules contain bulges, loops, and other features that distort helical regions, thus providing unique 3-D binding sites that can, in some cases, exhibit higher binding affinities to aminoglycosides as compared to analogous structures with less perturbed duplex regions (*11*, *12*). Given the therapeutic potential of targeting biologically relevant RNA sites, a number of groups have made semisynthetic aminoglycoside derivatives in an attempt to tune the RNA affinity, site specificity, and inhibition activities of the resulting derivatives (*13*−*17*). One potentially important RNA target for these compounds is the HIV Rev response element (RRE) (*18*).

The Rev−RRE interaction is essential to the replication of HIV (see ref *19* for a review). The Rev protein binds to the RRE and facilitates the export of viral RNA from the nucleus, while protecting it from the cell's splicing machinery (*19*). Without Rev−RRE binding, the proteins essential for virus production are never translated (*20*). The Rev binding site on the RRE is highly conserved across different groups of HIV-1 isolates, and is even similar to the RRE of HIV-2 (*18*, *21*). Compounds that inhibit HIV replication by binding to the RRE and displacing Rev are expected, therefore, to retain activity across genetically diverse HIV infections (*18*).

In 1993, Zapp et al. reported that certain aminoglycosides bind to the HIV-1 RRE and displace the Rev protein with moderate inhibitory activities (1 μM < IC_{50} < 100 μM) (*22*). Later studies by Hendrix et al. suggested that the most active aminoglycoside, neomycin B, binds nonspecifically to multiple sites on the RRE (*8*). In an attempt to improve the RRE affinity and specificity of aminoglycosides, we have made synthetic modifications to the aminoglycosides and evaluated the resulting derivatives for binding to the RRE (*23*, *24*). In this contribution, we report the synthesis and characterization of six new aminoglycoside derivatives (see Supporting Information for details). The RRE affinity, specificity, and RNA versus DNA selectivity of these compounds are compared to the parent aminoglycosides as well as four previously published high affinity RNA ligands.

We have recently communicated the synthesis and characterization of a new neomycin B derivative, trivially named "neo-S-acridine" (compound **5**, Figure 1) (*23*). Rev peptide displacement experiments (conducted in the absence of other nucleic acids) indicated that neo-S-acridine binds at (or near) the Rev binding site on the RRE with an affinity similar to

[1] Abbreviations: RRE, Rev response element; CT DNA, calf thymus DNA; HIV, human immunodeficiency virus; HEPES, 4-(2-hydroxyethyl)-1-piperazineethanesulfonic acid; EDTA, ethylenediaminetetraacetic acid; TE, Tris-EDTA.

that of the Rev protein (K_d = ~2 nM) (*23*). Enzymatic footprinting experiments and native gel shift electrophoresis support this conclusion (*23*). To our knowledge, the binding between neo-S-acridine and the RRE is still the highest affinity interaction between a natural RNA molecule and a small synthetic ligand reported in the literature (*13*−*17*). Here we demonstrate that neo-S-acridine has a very *low* specificity for the RRE (relative to a Rev_{34-50} peptide). The RRE specificity of neomycin−acridine conjugates can, however, be improved by changing the linker length between the intercalator and the aminoglycosidic moiety. In addition, we compare the RRE affinity and specificity of aminoglycoside−acridine conjugates to two well-established families of RNA ligands: aminoglycoside antibiotics and their dimeric derivatives.

For the purposes of this discussion, the term "specificity" will be defined as the affinity (K_{eq}) of a molecule to the RRE, weighted by its average affinity to many other nucleic acid binding sites.

$$\text{specificity} = \frac{K_{eq}\,(\text{interaction of interest})}{\text{average } K_{eq}\,(\text{other sites of interaction})} \quad (1)$$

The reported specificity is, therefore, dependent on the selection of the "other" species used for the comparison. Whenever possible, a heterogeneous mixture of nucleic acids is used for the basis of comparison, so that the reported specificity is with respect to many different potential nucleic acid binding sites. A commercially available mixture of tRNAs ("$tRNA^{mix}$") provides a biologically relevant mixture of over 30 different pre- and mature tRNAs for a broad specificity comparison. The term "selectivity", on the other hand, will be used in a more limited fashion, where the binding affinities of a small molecule to two different nucleic acids are compared.

EXPERIMENTAL SECTION

Aminoglycoside Derivatives. Tobramycin (free base) was a generous gift of Meiji Seika Kaisha Ltd. (Japan) and used as received. Kanamycin A sulfate was purchased from Sigma and desalted using AG 1X-4 (BioRad) (OH^- form of the resin). Neomycin B was obtained from Sigma, and purified as described (*27*). See Supporting Information for the synthesis and characterization of neo-N-acridine, neo-C-acridine, tobra-N-acridine, kana-N-acridine, neo-N-neo, and tobra-N-tobra. See ref *23* for the synthesis of neo-S-acridine, and see ref *26* for the synthesis of neo−neo, tobra−tobra, and kanaA−kanaA. Serial dilutions of all stock solutions were made in buffer (20 mM sodium phosphate pH 7.5, 100 mM KCl, 3 mM $MgCl_2$, 1 mM EDTA) to minimize loss of these compounds onto pipet tips and plastic tubes.

RRE66. T7 RNA polymerase was utilized for "run-off" in vitro transcription with a complementary 83-nt DNA template as described (*28*). Transcription products were purified using denaturing PAGE, extraction, and multiple rounds of ethanol precipitation. The expected sequence of the 66-nt RNA transcript was verified by 5′ end labeling with ^{32}P and subsequent enzymatic digestions (RNase T1, A, and U2) (*23*). The molecular extinction coefficient (260 nm) for the RRE was calculated by a summation of the extinction coefficients of each nucleotide multiplied by the number of times it appears in the sequence ($A = 15\,400$ cm^{-1} M^{-1}, $G = 11\,700$ cm^{-1} M^{-1}, $C = 7300$ cm^{-1} M^{-1}, $U = 10\,100$ cm^{-1} M^{-1}) to obtain 741 400 cm^{-1} M^{-1} for the RRE66 (*23*). For this value to be accurate, the RRE must first be hydrolyzed before quantification (*29*). Since base hydrolysis produces free nucleotides, this calculated extinction coefficient does not need to make any assumptions regarding nearest neighbor base stacking interactions. Procedure for hydrolysis: 1 μL of RNA solution is added to 10 μL of 1 M NaOH and heated 90 °C for 10 min. The reaction is then quenched with 10 μL of 1 M HCl, diluted into 500 μL of 50 mM sodium phosphate pH 7.5, and its absorbance at 260 nm is measured. By comparing the UV−vis absorbance spectrum of the RRE before and after base hydrolysis, an extinction coefficient of 560 000 cm^{-1} M^{-1} has been determined for the nonhydrolyzed (native) form of RRE66 (*29*). The differences in RRE absorbance, upon base hydrolysis, were not taken into account in previous studies, resulting in about 25% lower calculated concentrations of RRE66 (*23*). Since the total concentration of RRE is instrumental to both K_d and K_i calculations, approximately 2-fold higher apparent affinities for both the RevFl−RRE, and the neo-S-acridine−RRE binding interactions were, therefore, previously reported (*23*).

Rev Peptides. The synthesis, purification, and quantification of RevFl and RevIA have been described in the Supporting Information section of ref *30*.

Calf Thymus (CT) DNA. Sonicated CT DNA was purchased, in solution, from Gibco BRL. Solutions were quantified (without base hydrolysis) using an extinction coefficient of 13 100 cm^{-1} M^{-1} per base pair (*31*).

Poly r[A]−poly r[U]. The RNA duplex heteropolymer poly r[A]−poly r[U] was purchased from Sigma, dissolved in 1× TE, and quantified (without base hydrolysis), using an extinction coefficient of 14 280 cm^{-1} M^{-1} per base pair (*31*).

$tRNA^{mix}$. A mixture of pre- and mature yeast tRNAs (containing over 30 different species) was purchased from Sigma (type X). Stock solutions were prepared in 1× TE and quantified (after base hydrolysis as described above) using an extinction coefficient of 11 125 cm^{-1} M^{-1} per base (average of A, T, C, G). Stocks of $tRNA^{mix}$ can be quantified in its native form (without base hydrolysis) using an extinction coefficient of 9640 cm^{-1} M^{-1} per base (*29*).

Conditions for Binding Assays. All experiments were conducted at 22 °C in a buffer containing 30 mM HEPES (pH 7.5), KCl (100 mM), sodium phosphate (10 mM), NH_4-OAc (20 mM), guanidinium HCl (20 mM), $MgCl_2$ (2 mM), NaCl (20 mM), EDTA (0.5 mM), and Nonidet P-40 (0.001%). This complex mixture of cations and anions minimizes the nonspecific binding of ligands to the Rev−RRE complex, and maximizes the reversibility of the Rev−RRE interaction (as evident in both anisotropy and solid-phase assays). In addition, the loss of polycationic ligands (including RevFl, the dimers, and the acridine conjugates) onto pipet tips, cuvettes, etc., is minimized in this buffer.

RevFl−RRE66 Binding by Fluorescence Anisotropy. In a Perkin-Elmer LS-50B luminescence spectrometer equipped with polarizing filters, a 10 nM solution of RevFl in buffer was excited at 490 nm, and its emission monitored at 530 nm. Maximum slit widths and a G_f value of 1.006 were used for taking at least six independent anisotropy values for each

data point. RRE66 was then titrated into the RevFl solution and the anisotropy of RevFl was measured after each addition of RNA. Upon binding the RRE, only minor changes in the emission spectrum of fluorescein were seen (about 10% quenching of RevFl). We have, therefore, taken the change in anisotropy as being directly proportional to the fraction of RevFl bound. Nonlinear curve fitting of the RevFl association data (conducted as described in ref *23*) was used to fit the raw binding isotherm to a $K_d = 5 \pm 1$ nM (error indicates the standard deviation of the data for 3 individual titrations). This value is 2-fold higher than that previously reported (*23*), due to changes in the methodology used to quantify RRE stock solutions (discussed above under "*RRE66*").

RevFl Displacement Experiments by Fluorescence Anisotropy. A RevFl−RNA complex was formed by mixing RevFl and RRE66 (10 nM each) in a thermocontrolled fluorescence cuvette. Small volumes of a concentrated solution of inhibitor were then titrated while the fluorescence anisotropy of the solution was monitored (as described above). For all titrations, the final volume in the cuvette never increased by more than 5%. Nonlinear curve fitting was used to determine IC_{50} values by fitting the raw displacement data to a one-phase exponential decay curve using Prism 3.0, and allowing ΔA, A_F, and IC_{50} to float in the following equation:

$$A = \Delta A \exp^{((-0.69/IC_{50})C)} + A_F \qquad (2)$$

where A is the anisotropy value, ΔA is the difference between the initial anisotropy value and the final anisotropy value (A_F), C is the total concentration of inhibitor, and IC_{50} is the concentration of inhibitor where $A = (1/2\ \Delta A) + A_F$.

K_i values have been calculated from IC_{50} values by considering the following 3-way binding isotherm and the resulting equation:

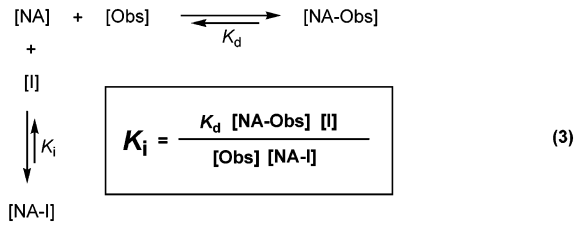

where [NA] is the concentration of "free" (unbound) nucleic acid, [Obs] is the concentration of the "free" observable species (either RevFl, or ethidium), [NA-Obs] is the concentration of the NA-Obs complex, [I] is the concentration of "free" inhibitor, and [NA-I] is the concentration of inhibitor-bound nucleic acid. According to the RevFl−RRE association curve, upon mixing 10 nM of RRE66 with 10 nM of RevFl, the concentration of RevFl−RRE complex [NA-Obs] = 5.0 nM, and the concentrations of free RRE and free RevFl ([NA] and [Obs]) are each 5.0 nM. Upon titration of the inhibitor to its IC_{50} value, the concentration of the complex [NA-Obs] = 2.5 nM, [Obs] = 7.5 nM, [NA] = 1.0 nM, [NA-I] = 6.5 nM, and the concentration of free inhibitor [I] = ((IC_{50} value) − [NA-I]). These values were used to solve eq 3, resulting in $K_i = ((IC_{50} - 6.5\ \text{nM})/4)$. This assumes that a single equivalent of inhibitor is sufficient to displace RevFl. The calculations for both K_i and K_d are critically dependent on the total concentration of RRE present, but the resulting K_i values for all compounds were approximately the same at 10-fold higher concentrations of RRE66 (*29*).

Solid-Phase Assay. Experiments were conducted as described in ref *30*. Briefly, beaded agarose covalently modified with stretavidin ("ImmunoPure") was purchased from Pierce and washed with 3 volumes of buffer (above). Dilute biotinylated RRE66 (500 μL of a 400 nM solution in buffer) was added to 1 mL of a 40% slurry (400 μL of beads and 600 μL of buffer). The slurry was incubated at room temperature for 1.5 h with constant inversion for mixing. By monitoring absorbance of the supernatant at 260 nm, the efficiency of RRE immobilization is calculated. The loading efficiency is >95% for biotinylated RRE and <1% for nonbiotinylated RRE. Following RRE immobilization, 1 equiv of RevFl was added, incubated for 1 h while mixing, and the supernatant quantified for fluorescence intensity. Under these conditions, approximately 80% of RevFl is associated with the solid support, and nonspecific binding of RevFl to the solid support is not observed (as determined by addition of RevFl to streptavidin-agarose which lacks immobilized RRE). Inhibition assays were conducted in 0.75 mL siliconized tubes, where 200 μL of buffer (above) was added, followed by 30 μL of the 30% Rev-RRE solid-phase slurry (at 0.5 pmol of RRE/μL of gel). A small volume of concentrated inhibitor and/or competitor was then added, mixed gently, and incubated at room temperature for 90 min with constant inversion for mixing. The tube was then gently centrifuged (1000 rpm for 30 s) to settle the beads. A total of 200 μL of supernatant was then added to 800 μL of "quantification buffer" (4 M guanidinium HCl, 250 mM Tris/HCl pH 9.0, 250 mM KCl, 50 mM $MgCl_2$, 0.01% Nonidet P-40), and quantified for fluorescence intensity (Perkin-Elmer LS-50B fluorimeter, maximum slit widths, Excitation 490 nm). For the maximum signal control (see Supporting Information for a representative titration), 200 μL of 8 M guanidinium HCl was added instead of buffer. For experiments containing CT DNA, 115 μM (final concentration in base pairs) of sonicated CT DNA was included. For experiments containing $tRNA^{mix}$, 230 μM (final concentration in bases) was included.

Ethidium Association. A 1.25 μM solution of ethidium bromide was excited at 546 nm, and its fluorescence emission was monitored at 600 nm while small aliquots of a concentrated nucleic acid were titrated. The fractional change in emission intensity was taken as equal to the fraction of ethidium bound and was used to calculate the concentration of free ethidium [C_f] and concentration of bound ethidium [C_b] at each concentration of nucleic acid [N_t] (total concentration). The data collected from 0.1 to 0.9 fractional change in emission intensity were then used to generate a Scatchard plot where r/C_f is plotted versus r, (where $r = [C_b]/[N_t]$). The negative inverse slope of this linear correlation is equal to K_d, and the X-intercept equals the binding stoichiometry (in equivalents of ethidium per base pair) (*32*).

Ethidium Displacement. The fluorescence intensity of a 1.25 μM solution of ethidium bromide was monitored (as above), and 300 nM (in bp) of either CT DNA or poly r[A]−r[U] RNA were added, followed by small aliquots of a concentrated inhibitor. IC_{50} values were determined by using eq 2 for curve-fitting the raw data (using fluorescence intensity instead of anisotropy). Under these conditions, no

significant increase in emission intensity was observed for ethidium upon addition of $tRNA^{mix}$. This prevents the application of ethidium displacement assays to evaluate the binding of $tRNA^{mix}$. The fluorescence intensity of ethidium does increase upon binding the RRE66 (*18*), but ethidium has at least two nonequivalent binding sites on the RRE (*18*), complicating the interpretation of displacement experiments using the RRE. Ethidium displacement experiments using tRNA and the RRE are, therefore, not presented. K_i values have been estimated from IC_{50} values by using the measured ethidium binding affinity and stoichiometry of each nucleic acid in conjunction with eq 3.

According to the ethidium−poly r[A]−r[U] association curve, the $K_d = 0.6$ μM, and the binding stoichiometry is 0.2 ethidium binding sites per base pair. Upon adding 300 nM of poly r[A]−r[U] to 1.25 μM of ethidium, therefore, the concentration of ethidium−RNA complex [NA-Obs] = 0.040 μM, free ethidium [Obs] = 1.21 μM, and free RNA [NA] = 0.020 μM (in available binding sites). Upon titration of the inhibitor to its IC_{50} value, the concentration of RNA−ethidium [NA-Obs] = 0.020 μM, free ethidium [Obs] = 1.23 μM, free RNA [NA] = 0.010 μM (in available binding sites), [NA-I] = 0.030 μM, and the concentration of free inhibitor [I] = ((IC_{50} value) − [NA-I]). Using these values to solve eq 3, K_i = ((IC_{50} − 30 nM)/3.1). This calculation assumes that one equivalent of inhibitor displaces one equivalent of ethidium.

According to the ethidium−CT DNA association curve, the $K_d = 2.4$ μM, and the binding stoichiometry is 0.2 ethidium binding sites per base pair. Upon adding 300 nM of CT DNA to 1.25 μM of ethidium, the concentration of ethidium-DNA [NA-Obs] = 0.020 μM, free ethidium [Obs] = 1.23 μM, and free DNA [NA] = 0.040 μM (in available binding sites). Upon titration of the inhibitor to its IC_{50} value, the concentration of the complex [NA-Obs] = 0.010 μM, free ethidium [Obs] = 1.24 μM, free RNA [NA] = 0.020 μM (in available binding sites), [NA-I] = 0.030 μM, and the concentration of free inhibitor [I] = ((IC_{50} value) − [NA-I]). Using these values to solve eq 3, K_i = ((IC_{50} − 30 nM)/1.6). This calculation assumes that one equivalent of inhibitor displaces one equivalent of ethidium and, thus, the term "apparent" affinity is used.

RESULTS

Rev−RRE Association and Inhibition According to Fluorescence Anisotropy. The fluorescence anisotropy of a fluorescein-labeled Rev_{34-50} peptide "RevFl" has been used to monitor to the real-time association and subsequent inhibition of the Rev−RRE interaction (*18*, *33*, *34*). Upon titration of the RRE into a buffered solution of RevFl (Figure 2), an increase in RevFl anisotropy is observed that reflects the formation of a RevFl−RRE complex (Figure 3 A). Analysis of these data yields an affinity of 5 ± 1 nM for RevFl−RRE binding (*35*). This value is similar to the values reported for the binding of the RRE by related Rev peptides (*33*−*34*), as well as the Rev protein (*25*). Once the RevFl−RRE complex is formed, an inhibitor can be titrated and the displacement of RevFl from the RRE is apparent by a decrease in the anisotropy of RevFl back to the value of the free peptide in solution (Figure 3B). The RevFl−RRE IC_{50}

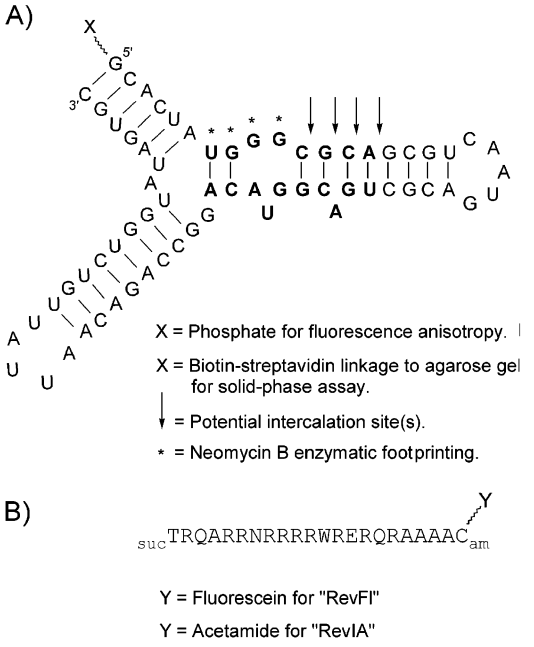

FIGURE 2: (A) Secondary structure of the 66 nucleotide HIV-1 RRE construct "RRE66". The high-affinity Rev binding site is indicated in bold (*19*). Also indicated is the enzymatic footprinting of neomycin B (∗) (*22*), as well as the potential high-affinity binding sites for intercalating agents (arrows) (*41*). (B) Sequence of the peptides "RevFl" and "RevIA" based upon Rev_{34-50}, where $_{suc}$ = succinylated, and $_{am}$ = amidated.

values for the aminoglycosides and their derivatives (**1**−**13**) as well as RevIA (**14**) are summarized in Table 1a. If a single binding site for the small molecule is responsible for the displacement of RevFl, its affinity at or near Rev binding site on the RRE can be calculated from the IC_{50} value (where K_i is equivalent to K_d) (*23*, *33*). The apparent RRE affinities of compounds **1**−**14** are summarized in Table 1b. The term "apparent" is used since the 1:1 displacement stoichiometries are, for most molecules, unproven. This assumption does hold true for **14** and has also been validated for neo-S-acridine (*23*, *29*). We have examined the validity of this assumption for all other compounds by measuring the K_i value for each compound at 10 and 100 nM of RRE66 (*29*). While the IC_{50} values for each compound are different at each concentration of RRE, the calculated K_i values are approximately the same, thus supporting a 1:1 displacement stoichiometry for all compounds presented (*29*). All of the modified aminoglycosides (including all of the acridine−aminoglycoside conjugates and the aminoglycoside dimers) bind at (or near) the Rev binding site of the RRE with a very high apparent affinity of ($K_i \leq 10$ nM, Table 1b). The RRE specificity of these compounds, however, is highly variable.

Measuring RRE Specificity Using a Solid-Phase Assay. To evaluate the RRE specificity of each compound, its affinity to other nucleic acids must be measured (eq 1). Two orthogonal fluorescence-based methods have been employed for this purpose. We recently communicated a novel solid-phase assay that can rapidly evaluate the RRE specificity of small molecules (*30*). The assay is based on the release of RevFl from a solid-phase immobilized RRE66. Inhibitory ligands that bind at or near the Rev binding site on the RRE will displace RevFl from the solid support into solution. The

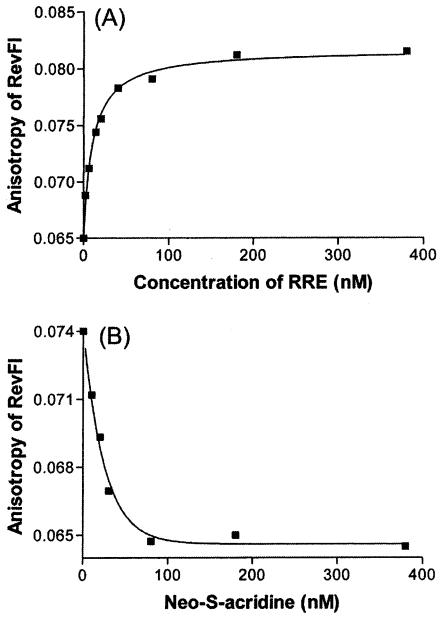

FIGURE 3: Fluorescence anisotropy is used to monitor RevFl−RRE association (A), and dissociation by a competitive inhibitor (B). The fluorescence anisotropy of 10 nM of RevFl is monitored as RRE66 is titrated (A). Upon partial complex formation (10 nM of RRE), an inhibitor is added (neo-S-acridine) that displaces RevFl from the RRE (B). The shape of the displacement isotherm is approximately the same for all compounds evaluated. All binding experiments (including those using the solid-phase assay and ethidium displacement) were conducted at 22 °C in a buffer containing 30 mM HEPES (pH 7.5), KCl (100 mM), sodium phosphate (10 mM), NH_4OAc (20 mM), guanidinium HCl (20 mM), $MgCl_2$ (2 mM), NaCl (20 mM), EDTA (0.5 mM), and Nonidet P-40 (0.001%). This complex mixture of cations and anions is found to minimize aggregation and maximize the reversibility of the Rev−RRE interaction (as evident in both anisotropy and solid-phase assays).

emission intensity of the solution is then measured to quantify the fractional inhibition of RevFl binding. RevFl binds to the immobilized RRE with the same affinity as in solution, and shows no binding to agarose/strepavidin gel that lacks immobilized RRE (*30*). As in solution, RevFl binds to the immobilized RRE with high specificity, and it is not significantly displaced by a large excess (100-fold) of $tRNA^{mix}$ or CT DNA (*30*). The IC_{50} values of inhibitors can, therefore, be determined in either the absence or presence of an excess of competing nucleic acids by measuring the concentration-dependent release of RevFl from the immobilized RRE66 (see Supporting Information for a representative titration using neomycin B, and Table 2 for a summary of IC_{50} values). The change in activity of each inhibitor, upon addition of a competitor nucleic acid, is proportional to its affinity for that competitor. Dividing the average IC_{50} values measured in the presence of nucleic acid competitors by the IC_{50} values measured in the absence of other nucleic acids, a "specificity ratio" is calculated for each compound (Table 2d). The lower this ratio is, the more specific the ligand is for the RRE. This ratio is, however, somewhat sensitive to the total concentration of competing nucleic acids relative to the IC_{50} of each compound. Less active compounds, including the aminoglycosides, are less affected by the presence of competitors since their IC_{50} values are sometimes *higher* than the concentrations of competitor nucleic acids used (hence, even if a competitor becomes saturated with the inhibitor, the Rev−RRE IC_{50} value may not appreciably change). The absolute RRE *specificity* of each compound is, therefore, a combination of both the RRE specificity ratio and its absolute affinity for the RRE. It should be noted that the IC_{50} values presented for Rev−RRE inhibition are not directly comparable between Tables 1 and 2 because IC_{50} values (unlike K_i values) are highly dependent upon the concentrations of components being inhibited. These parameters are not easily determined for the solid-phase assay. Despite this, the *trends* in Rev−RRE IC_{50} values are the same for both fluorescence anisotropy (Table 1a) and solid-phase displacement experiments (Table 2a).

Ethidium Displacement Experiments. To provide an orthogonal, and somewhat more direct approach, for evaluating RRE specificity, we have used ethidium bromide displacement experiments to measure the apparent affinity of each compound for duplex DNA and RNA (*39*, *40*). The fluorescence emission intensity of ethidium bromide increases upon addition of either CT DNA or poly r[A]−r[U] duplex RNA (Figure 4 A). The fraction of ethidium bound as a function of nucleic acid concentration can, therefore, be

Table 1: RevFl−RRE IC_{50} Values from Fluorescence Anisotropy (a), Calculated RRE Affinities (K_i) (b), and Ethidium Displacement IC_{50} Values and Apparent Affinities (K_i) for poly r[A]−r[U] Duplex RNA (c) and (d), and CT DNA (e) and (f)[a]

compound	(a) RevFl−RRE66 IC_{50}[b] (μM)	(b) apparent RRE66 affinity K_i (M)	(c) ethidium + poly r[A]−r[U] IC_{50}[c] (μM)	(d) apparent r[A]−r[U] affinity K_i (M)	(e) ethidium + CT DNA IC_{50}[c] (μM)	(f) apparent CT DNA affinity K_i (M)
neomycin B (**1**)	0.9	2.2×10^{-7}	6.0	1.9×10^{-6}	60	3.8×10^{-5}
tobramycin (**2**)	10	2.5×10^{-6}	25	8.1×10^{-6}	>800	$>5.00 \times 10^{-4}$
kanamycin A (**3**)	100	2.5×10^{-5}	450	1.5×10^{-4}	>15000	$>9.4 \times 10^{-3}$
neo-N-acridine (**4**)	0.016	2.4×10^{-9}	0.65	2.0×10^{-7}	0.85	5.1×10^{-7}
neo-S-acridine (**5**)	0.017	2.6×10^{-9}	0.05	6.5×10^{-9}	0.14	6.9×10^{-8}
neo-C-acridine (**6**)	0.017	2.6×10^{-9}	0.13	3.2×10^{-8}	0.08	3.1×10^{-8}
tobra-N-acridine (**7**)	0.030	5.9×10^{-9}	1.3	4.1×10^{-7}	0.49	2.9×10^{-7}
kanaA-N-acridine (**8**)	0.045	9.6×10^{-9}	4.4	1.4×10^{-6}	2.1	1.3×10^{-6}
neo−neo (**9**)	0.017	2.6×10^{-9}	0.067	1.2×10^{-8}	0.65	3.9×10^{-7}
neo-N-neo (**10**)	0.015	2.1×10^{-9}	0.035	1.6×10^{-9}	0.45	2.6×10^{-7}
tobra−tobra (**11**)	0.040	8.4×10^{-9}	0.61	1.9×10^{-7}	1.0	6.1×10^{-7}
tobra-N-tobra (**12**)	0.043	9.1×10^{-9}	0.47	1.4×10^{-7}	1.5	9.2×10^{-7}
kanaA−kanaA (**13**)	0.050	1.1×10^{-8}	6.0	1.9×10^{-6}	12.0	7.5×10^{-6}
RevIA (**14**)	0.014	1.9×10^{-9}	1.0	3.1×10^{-7}	1.3	7.9×10^{-7}

[a] Experimental errors are less than or equal to ± 35% of each value. [b] Using 10 nM each of RRE66 and RevFl. [c] 1.25 μM of ethidium bromide + 300 nM (base pairs) of the duplex nucleic acid.

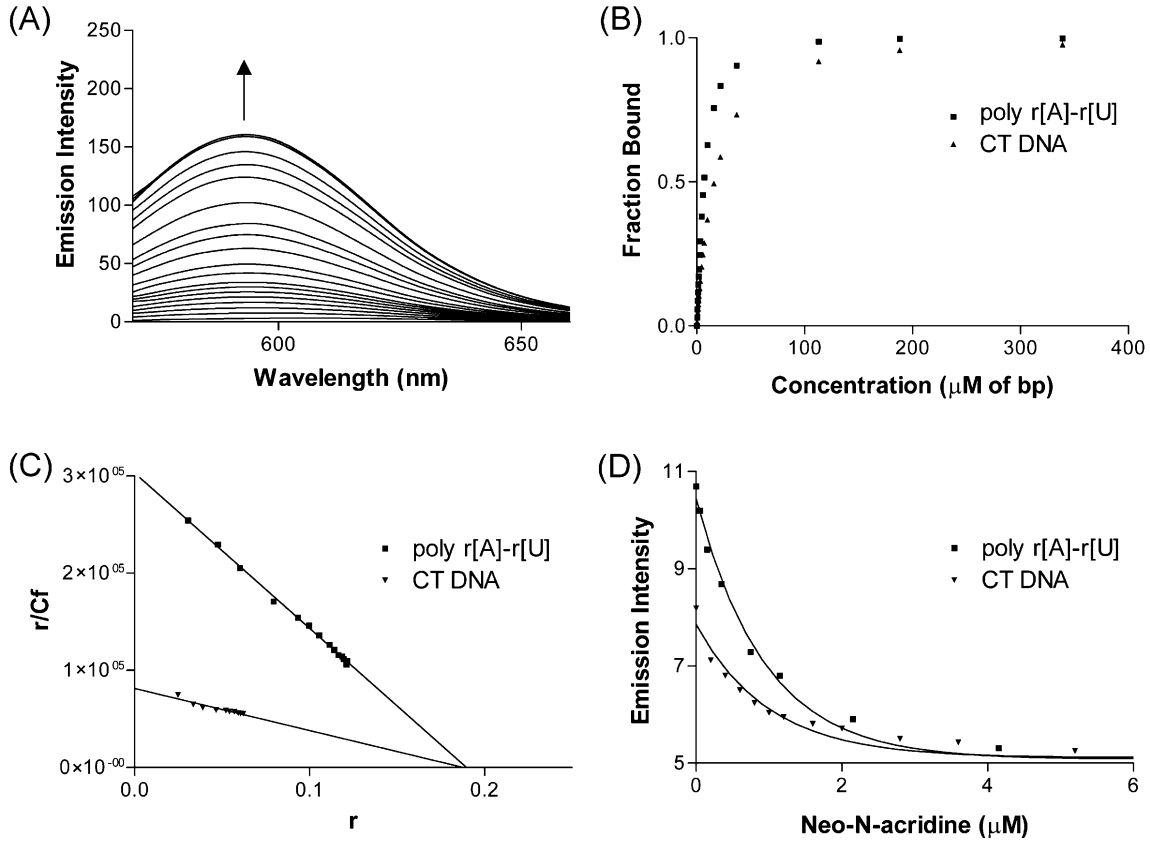

FIGURE 4: Increasing fluorescence intensity of a 1.25 μM solution of ethidium bromide (excitation 546 nm) upon addition of poly r[A]−r[U] (A). Fraction of ethidium bound as a function of nucleic acid concentration (B) as determined by the fluorescence emission intensity at 600 nm. Scatchard plot for the binding of ethidium by poly r[A]−r[U] and CT DNA (C). Examples of ethidium displacement experiments from poly r[A]−r[U] and CT DNA using neo-N-acridine (D).

Table 2: IC_{50} Values According to Solid-Phase Assay[a]

compound	(a) IC_{50} (μM) without competitors	(b) IC_{50} (μM) with CT DNA[b]	(c) IC_{50} (μM) with $tRNA^{mix}$ [c]	(d) RRE specificity ratio[d]
neomycin B (**1**)	7	8	20	2.0
tobramycin (**2**)	45	48	100	1.6
kanamycin A (**3**)	750	750	1200	1.3
neo-N-acridine (**4**)	0.040	0.15	1.2	17
neo-S-acridine (**5**)	0.040	0.45	1.6	26
neo-C-acridine (**6**)	0.040	1.7	2.3	50
tobra-N-acridine (**7**)	0.24	4.0	2.8	14
kanaA-N-acridine (**8**)	0.61	2.5	2.2	3.9
neo−neo (**9**)	0.050	0.11	4.8	49
tobra−tobra (**11**)	0.13	0.20	2.6	11
kanaA−kanaA (**13**)	0.24	0.60	2.5	6.5
RevIA (**14**)	0.035	0.080	0.085	2.3

[a] Experimental errors are less than or equal to ± 35% of each value. [b] 115 μM (base pairs) of CT DNA included. This is approximately a 100-fold molar excess of bases relative to the RRE. [c] 230 μM (bases) of a tRNA mixture (Sigma type X) included. This is approximately a 100-fold molar excess of bases relative to the RRE. [d] Specificity ratio = (average IC_{50} in the presence of DNA and $tRNA^{mix}$)/(IC_{50} in the absence of other nucleic acids).

determined (Figure 4B). Scatchard analysis of these data (Figure 4C) indicates that, under these conditions, ethidium has approximately the same binding stoichiometry for these two nucleic acids (0.2 equiv of ethidium per base pair). Consistent with earlier studies (*31*), ethidium has approximately a 4-fold higher affinity to poly r[A]−r[U] duplex RNA (K_d = 0.6 μM) as compared to CT DNA (K_d = 2.4 μM) (Figure 4C). Upon titration of another ligand, ethidium is displaced from each nucleic acid, and its fluorescence intensity decreases back to its value in solution (see Figure 4D for representative examples). The concentration of each compound **1**−**14** needed to displace one-half of the ethidium from either CT DNA or poly r[A]−r[U] duplex RNA is reported in Table 1. The IC_{50} values for ethidium and RevFl displacement are not directly comparable between columns a, c, and e of Table 1, since IC_{50} values (unlike K_i values) are highly sensitive to the affinities and concentrations of the components being inhibited. To make these IC_{50} values more comparable, apparent affinities (K_i) have been calculated by assuming a single equivalent of ethidium is displaced by each equivalent of inhibitor (Table 1d,f). Assumptions made regarding the binding and displacement stoichiometries of these interactions may affect the absolute magnitudes of the reported affinities (Table 1b,d,f), but the relative trends in the activities of these compounds will be unaffected (Tables 1a,c,e, and 2). By comparing the trends in the nucleic acid affinity and specificity of individual compounds (or families of compounds), the rules that govern aminoglycoside-mediated recognition of DNA and RNA can be assessed.

Affinity and Specificity of Unmodified Aminoglycosides. Consistent with the trends reported in earlier studies (*9*, *24*) the unmodified aminoglycosides (**1**−**3**) have, in general, a higher affinity to RNA as compared to DNA. Neomycin has

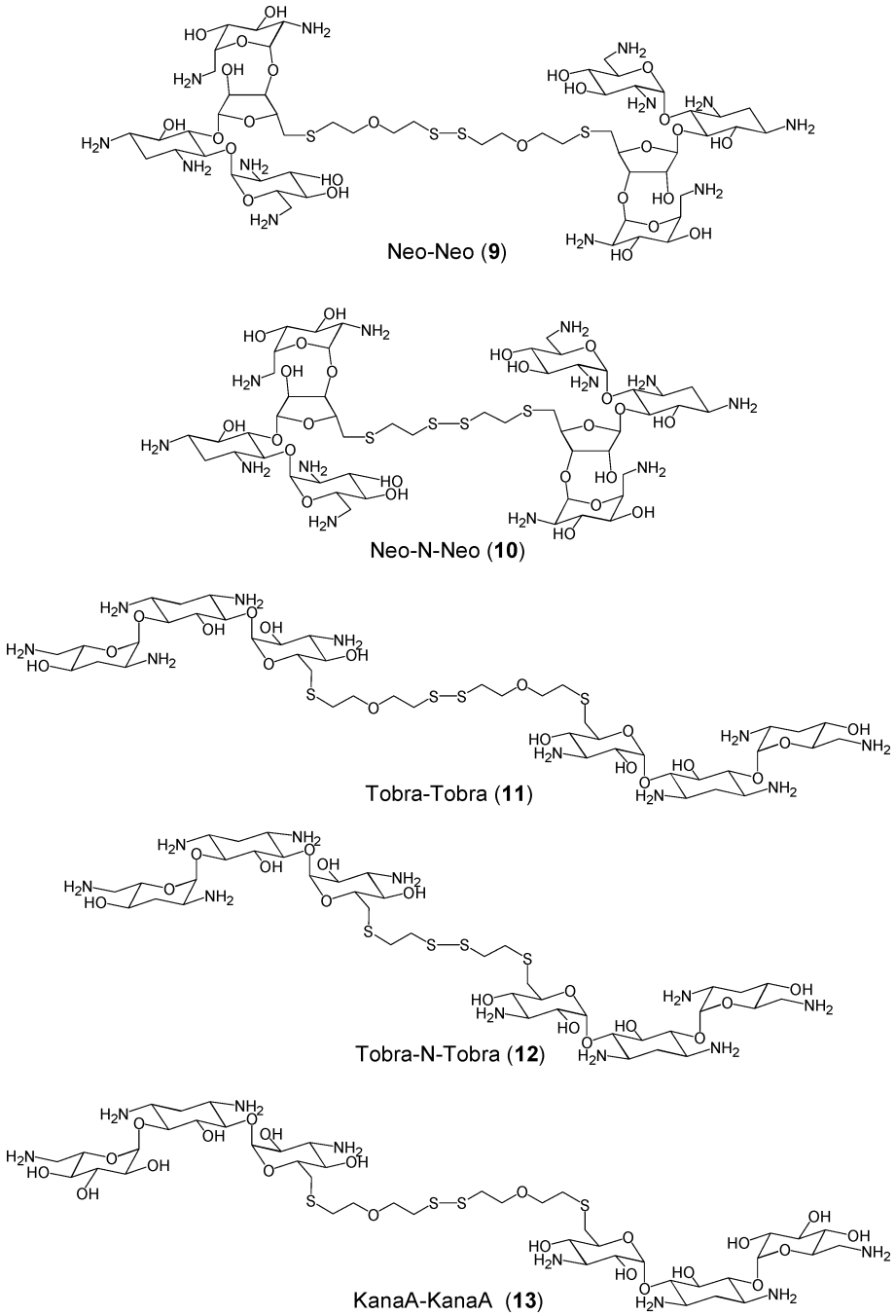

FIGURE 5: Structures of dimeric aminoglycosides. See Supporting Information for the synthesis and characterization of **10** and **12**.

about a 20-fold higher affinity to poly r[A]−r[U] as compared to CT DNA (Table 1d,f). Tobramycin and kanamycin A each have over a 60-fold higher affinity to poly r[A]−r[U] as compared to CT DNA, and therefore, exhibit more RNA selectivity than neomycin B. Results from the solid-phase assay are similar, where each aminoglycoside (especially neomycin B) loses more activity in the presence of $tRNA^{mix}$ than in the presence of CT DNA (Table 2). Similar results are obtained in the presence of poly r[A]−r[U] RNA and plasmid DNA (*24*). This supports, in general, a very broad RNA over DNA selectivity by the aminoglycosides.

Consistent with earlier studies (*11*, *18*, *36*, *37*, *38*), neomycin B binds to the RRE with an apparent affinity of approximately 0.2 μM (Table 1b). Tobramycin has about a 10-fold lower RRE affinity than neomycin B, and kanamycin A has about a 10-fold lower affinity than tobramycin (Table 1b). These differences are consistent with the binding of these compounds to an A-site hairpin, where each additional amino group increases its RNA affinity by approximately 10-fold (*44*).

Consistent with an earlier report (*11*), neomycin B has a higher affinity to the RRE as compared to unperturbed duplex RNA. According to RevFl and ethidium displacement experiments, neomycin B (**1**) has about a 10-fold higher affinity to the RRE as compared to poly r[A]−r[U] (Table 1b,d). Tobramycin, on the other hand, has only a 3-fold higher affinity to the RRE than poly r[A]−r[U], and kanamycin A has approximately a 15-fold higher affinity to the RRE than poly r[A]−r[U] (Table 1). These results are

consistent with differences in Rev−RRE inhibition activities of these three compounds when the solid-phase assay is conducted in the presence or absence of poly r[A]−r[U] RNA (*24*), and support a moderate, yet general, preference of the aminoglycosides for the RRE versus simple duplex RNA.

Affinity and Specificity of Neomycin−Acridine Conjugates and RevIA. Consistent with our initial report (*23*, *35*), both neo-S-acridine (**5**) and the unlabeled Rev peptide "RevIA" (**14**) have approximately the same affinity for the Rev binding site on the RRE (K_i = ∼2 nM) (Tables 1b and 2). In the presence of CT DNA or $tRNA^{mix}$, however, the activity of neo-S-acridine drops by 10- and 40-fold, respectively (Table 2). Under these same conditions, the IC_{50} values for the unlabeled Rev peptide drop by only 2−3-fold (Table 2). This indicates that neo-S-acridine has a much higher affinity to these competing nucleic acids as compared to RevIA, and therefore, a much lower RRE specificity (eq 1). Ethidium displacement experiments provide similar results. Neo-S-acridine has a 10-fold higher affinity to poly r[A]−r[U] than CT DNA, and it has much higher affinity to both of these nucleic acids as compared to RevIA (Table 1d,f). Importantly, the unlabeled Rev peptide (**14**) exhibits almost a 200-fold higher affinity to the RRE as compared to poly r[A]−r[U] (Table 1b,d). Neo-S-acridine (**5**), on the other hand, exhibits only a 2-fold higher affinity to the RRE as compared to poly r[A]−r[U] duplex RNA (Table 1). This is a lower RRE selectivity than that observed for the parent compound, neomycin B. Taken together, these results indicate that the RNA over DNA selectivity of neo-S-acridine is largely maintained by the conjugate, but that the RRE specificity of neo-S-acridine (with respect to other RNAs) is very poor. Both of these properties, however, vary as a function of linker-length.

We have synthesized two new neomycin−acridine conjugates with different linker lengths (compounds **4** and **6**, Figure 1) and evaluated their RRE affinity and specificity. Neo-N-acridine (**4**) has a shorter linker than neo-S-acridine, but both compounds have approximately the same affinity for the Rev binding site of the RRE (Tables 1 and 2). In contrast to neo-S-acridine (**5**), neo-N-acridine (**4**) retains much more of its activity in the presence of a vast excess of CT DNA and $tRNA^{mix}$ (Table 2). Consistent with this finding, ethidium displacement experiments indicate that neo-N-acridine (**4**) has much lower affinities to CT DNA and poly r[A]−r[U] RNA (7- and 30-fold lower affinities, respectively) as compared to neo-S-acridine (Table 1d,f). Neo-N-acridine has almost a 100-fold higher affinity to the RRE as compared to poly r[A]−r[U] (Table 1b,d), and it exhibits the best RRE specificity ratio (lowest value) as compared to all the other neomycin derivatives evaluated (compounds **4**, **5**, **6**, and **9**, Table 2d).

Interestingly, all of the three neomycin−acridine conjugates (**4**−**6**) have (within experimental error) the same RRE affinity (Tables 1 and 2). These compounds, however, have different RRE specificity ratios (Table 2d). Neo-N-acridine has the shortest linker length and the best RRE specificity, neo-C-acridine has the longest linker and the worst specificity, and neo-S-acridine has an intermediate linker length and an intermediate RRE specificity (Table 2d). Ethidium bromide displacement experiments support this trend and indicate that neo-S-acridine binds to simple duplex RNA (poly r[A]−r[U]) and CT DNA with high apparent affinities (K_i = 6 and 70 nM, respectively). Neo-C-acridine, as compared to neo-S-acridine, has a lower affinity to poly r[A]−r[U], but a higher affinity to CT DNA with K_i = 32 and 31 nM, respectively (Table 1d,f). Neo-N-acridine, on the other hand, has a much lower affinity to both of these nucleic acids with K_i = 200 and 510 nM for poly r[A]−r[U]) and CT DNA, respectively. Taken together, these results indicate that the RRE specificity of these neomycin−acridine conjugates is inversely proportional to their linker length, and that RNA over DNA selectivity of each conjugate is highly sensitive to linker length.

Affinity and Specificity of Acridine Conjugates of Kanamycin and Tobramycin. We have conjugated aminoacridine to the 6″ position of both tobramycin and kanamycin A to provide the new aminoglycoside-acridine conjugates "tobra-N-acridine" (**7**) and "kanaA-N-acridine" (**8**). RevFl displacement experiments indicate that **7** and **8** have approximately 400- and 2500-fold higher RRE affinities, respectively, as compared to their "parent" aminoglycosides (Table 1b). In contrast, the conjugation of acridine to neomycin B increases its affinity to the RRE by approximately 100-fold (Table 1). Interestingly, neither **7** nor **8** exhibit a general selectivity for RNA over DNA. These compounds, in fact, have slightly higher affinities to CT DNA as compared to both poly r[A]−r[U] and $tRNA^{mix}$ (Tables 1d,f, and 2a−c). This is the opposite trend as exhibited by neo-N-acridine (**4**). Interestingly, the unlabeled Rev peptide is highly specific for the RRE, but, in general, it is not very selective for RNA over DNA (Tables 1 and 2). It appears, therefore, that high RNA selectivity is not a prerequisite for high RRE specificity. Consistent with this, the kanamycin A- and tobramycin−acridine conjugates exhibit better RRE specificity ratios than the neomycin−acridine conjugates, but little if any RNA over DNA selectivity (Tables 1 and 2).

All aminoglycoside−acridine conjugates (**4**−**8**) exhibit a high affinity for the RRE (K_i < 10 nM, Table 1b). The solid-phase assay indicates, however, that compared to all other acridine conjugates kanaA-N-acridine has the best RRE specificity ratio (Table 2d). Consistent with this, ethidium displacement experiments (Table 1) confirm that kanaA-N-acridine has a relatively low affinity to both CT DNA and poly r[A]−r[U] (K_i = ∼1 μM). Neo-N-acridine and tobra-N-acridine, on the other hand, bind to these nucleic acids with much higher affinities (Table 1) and exhibit lower RRE specificity ratios than kanaA-N-acridine (Table 2). Interestingly, the neomycin-based acridine conjugates have, in general, the highest RRE affinity and the lowest RRE specificity; the kanamycin A derivatives have a slightly lower RRE affinity and the best RRE specificity; and the tobramycin derivatives have both an intermediate affinity and specificity (Tables 1 and 2). A similar trend is also observed for the aminoglycoside dimers.

RRE Affinity and Specificity of Aminoglycoside Dimers. Dimerization dramatically increases the affinity of aminoglycosides to many different RNAs including the HH16 ribozyme (*26*), $tRNA^{Phe}$ (*6*), a dimerized A-site (*45*), the *Tetrahymena* ribozyme (*46*), and the RRE (Tables 1 and 2). Dimerization increases the binding affinity of aminoglycosides to both poly r[A]−r[U] and the RRE by up to 1000-fold depending on the identity of the aminoglycoside (Table 1). The dimerization of neomycin B increases its affinity to the RRE66, poly r[A]−r[U], *and* CT DNA by approximately

100-fold (compounds **1**, **9**, and **10**, Table 1). The dimeric neomycin B derivatives (**9** and **10**) have similar affinities ($K_i = 1-10$ nM) to both poly r[A]−poly r[U] and the RRE66 (Table 1). The solid-phase assay indicates that neo−neo (**9**) also has a high affinity to a mixture of tRNAs. In the presence of $tRNA^{mix}$ it loses about 100-fold of its Rev−RRE inhibitory activity (Table 2a,c). This unusually high general affinity for RNA gives rise to neo−neo's very poor RRE specificity ratio (Table 2d). Indeed, the neomycin dimers exhibit little if any preference for the RRE over simple duplex RNA (Table 1). Neomycin's RNA over DNA selectivity is, however, maintained upon dimerization. The neomycin dimers have 10−100 fold higher affinities to poly r[A]−r[U] duplex RNA as compared to CT RNA (Table 1), and the inhibitory activity of neo−neo decreases by only 2-fold in the presence of a vast excess of CT DNA (Table 2a,b).

Tobra−tobra (**11**) has a 300-fold higher affinity to the RRE when compared to the parent compound tobramycin (**3**) (Table 1). As observed for neo−neo, tobra−tobra retains most of its Rev−RRE inhibition activity in the presence of excess CT DNA and loses activity in the presence of other RNAs (Table 2). Compared to neo−neo, tobra−tobra has about a 3-fold lower RRE affinity (Tables 1 and 2), but it is about 2-fold *more* active for Rev-RRE inhibition in the presence of $tRNA^{mix}$ (Table 2). This indicates that tobra−tobra has a significantly higher specificity for the RRE as compared to neo−neo. Ethidium displacement experiments confirm that upon dimerization of tobramycin, about a 40-fold increase in affinity for simple duplex RNA is observed, which is much lower than the 300-fold increase in RRE affinity. The dimerization of neomycin B, on the other hand, increases its affinity to both the RRE and poly r[A]−r[U] by about the same factor (Table 1).

The dimerization of kanamycin A increases its affinity to the RRE by 2200-fold, and for poly r[A]−r[U] an increase of only 80-fold is observed (Table 1). Compared to all the aminoglycoside dimers evaluated, the kanaA−kanaA dimer (**13**) has the best RRE specificity ratio (Table 2). Ethidium displacement experiments confirm that, compared to all the high-affinity RRE ligands ($K_d \leq 10$ nM), the kanaA−kanaA dimer has the lowest affinity to simple duplex DNA and RNA (Table 1d,f). These trends are very similar to those observed for the aminoglycoside−acridine conjugates, where the conjugates with slightly lower RRE affinities typically exhibit better RRE specificities. Interestingly, the kanaA−kanaA dimer exhibits a 2-fold better Rev−RRE inhibitory activity in the presence of $tRNA^{mix}$ than does neo−neo, even though neo−neo has a 5-fold higher RRE affinity than does kanaA−kanaA (Tables 1 and 2). This illustrates the inherent difficulty of measuring RNA affinities in the presence of nonspecific competing nucleic acids, as the measurements can reflect the selectivity of the interactions, not necessarily the trends in affinity.

Linker lengths play a major role in the RRE specificity of the neomycin−acridine conjugates where shorter linkers provide higher RRE specificity (presented above). Neomycin B and tobramycin dimers were, therefore, synthesized with two different linkers (Figure 5). Unlike the trends observed for the neomycin−acridine conjugates with different lengths, we have not observed significant differences in the IC_{50} values for RevFl or ethidium bromide displacement for tobra−tobra (**11**) versus tobra−N-tobra (**12**), or for neo−neo (**9**) versus neo−N-neo (**10**) (Table 1). Neo−N-neo (**10**), however, possesses the same linker length as neo-C-acridine (**6**), allowing a direct comparison between the two compounds. Both the neomycin dimer and acridine conjugate (**10** and **6**, respectively) have approximately the same affinity for the Rev binding site on the RRE (Table 1). This suggests that both the neomycin and acridine moieties contribute approximately the same binding energy to the interaction between RRE66 and the neo-acridine conjugate.

DISCUSSION

Neomycin−Acridine Conjugates. Enzymatic footprinting experiments by Zapp et al. suggested that neomycin B binds near the purine-rich bulge on the RRE (*22*). Flanking this internal bulge is a single adenosine bulge (Figure 2). Intercalating agents are known to preferentially bind to duplex regions that contain single-base bulges (*41*). In an attempt to create an RRE ligand that will simultaneously recognize both the RRE's internal G-rich bulge as well as its single adenosine base-bulge, 9-aminoacridine was conjugated to the 5″ hydroxyl of neomycin B (*23*). Preliminary binding studies with compound **5** and the RRE were conducted using native gel shift electrophoresis and enzymatic footprinting experiments in the presence of a large excess of $tRNA^{mix}$ (*23*). These experiments showed that neo-S-acridine (**5**) binds within the Rev binding site of the RRE, and that it displaces a Rev peptide with about a 10-fold higher activity as compared to neomycin B (**1**) (*23*). This is the same difference between these compounds according to the solid-phase assay when RevFl displacement experiments are conducted in the presence of an excess of $tRNA^{mix}$ (Table 2c). In the absence of competing nucleic acids, however, neo-S-acridine inhibits Rev-RRE binding about 100-fold better than neomycin B (Tables 1a and 2a). The reason for this 10-fold difference is that neo-S-acridine binds to many nucleic acids (including CT DNA, poly r[A]−r[U], and $tRNA^{mix}$) with high affinity (Tables 1 and 2). The RRE specificity of neo-S-acridine can, however, be improved by shortening the linker between its two moieties.

All three neomycin−acridine conjugates **4**−**6** have approximately the same RRE affinity (Tables 1 and 2). The differences in their RRE specificity ratios are, therefore, directly proportional to their differences in RRE specificity (eq 1). An obvious trend in RRE specificity is observed for these three conjugates: the linker length is inversely proportional to their RRE specificity (Table 2d). Ethidium bromide displacement experiments confirm that, compared to neo-N-acridine, both neo-C-acridine and neo-S-acridine have higher affinities to simple duplex RNA and DNA (Table 1c−f). The short linker in neo-N-acridine may impose fewer degrees of freedom onto the conjugate and, therefore, fewer nucleic acids can bind to it with high affinity. Interestingly, the conjugate with a medium-length linker (neo-S-acridine) has the "optimal" linker length for binding to poly r[A]−r[U] duplex RNA (Table 1d). This may indicate that neo-N-acridine has "too short" of a linker for both the acridine and the neomycin moieties to bind to poly r[A]−r[U] simultaneously. On the other hand, the long linker of neo-C-acridine may impose a small entropic disadvantage for the simultaneous binding of both moieties to poly r[A]−

r[U]. Both the solid-phase assay and ethidium bromide displacement experiments indicate that neo-C-acridine (**6**) has the highest affinity to CT DNA, followed by neo-S-acridine (**5**), and finally neo-N-acridine (**4**) (Tables 1 and 2). The longer linker of neo-C-acridine may give DNA better "access" to the intercalating moiety, as neomycin B is an RNA-selective molecule and acridine is essentially a non-specific intercalating agent (*42*). These results indicate that both the RNA over DNA selectivity, and the RRE specificity of aminoglycoside intercalator conjugates is "tunable" by variation of linker length.

Tok et al. have also recently reported intercalator−glycoside conjugates with linkers of variable length (*43*). Their approach involved incorporation of methylene spacers to link the 6″ amine of paromomycin to either pyrene or thiazole orange. Subsequent evaluation of these compounds as A-site antagonists indicated that as the number of atoms in the linker increases, the A-site affinity decreases (*43*). This is markedly different than the trend observed here, as all of the neo-acridine conjugates have, within error, the same RRE affinity (Tables 1 and 2). In addition, the neo-acridine conjugates with longer linkers have *higher* affinities to duplex DNA and RNA. It is possible that hydrophobic linkers (including polymethylene chains) introduce a penalty for binding nucleic acids (*43*). Indeed, other groups have found that linker composition is an important determinant for RNA binding (*47*). Ethylene glycol and thioether linkers are neutral, but well-hydrated, flexible linkages that should not, by themselves, significantly interact with RNA. Indeed, we have evaluated the synthetic precursor of the neo−neo dimer (**9**) that has a glycol linker attached at the 5″ hydroxyl of neomycin (see Supporting Information for synthesis and structure of 5″-β-mercaptoethylether-neomycin B). This "linker-only" neomycin B conjugate has approximately the same RRE affinity (K_i = 150 nM) as unmodified neomycin B (K_i = 220 nM). This indicates that the position and composition of this particular linker does not, in itself, dramatically affect the RRE affinity of the resulting conjugates.

Tobramycin and Kanamycin−Acridine Conjugates. Compared to Neo-N-acridine, kanaA-N-acridine (**8**) has a slightly lower RRE affinity, but it exhibits a better RRE specificity. Tobra-N-acridine (**7**) has an RRE affinity and specificity that are intermediate between the neo-acridine conjugates and kanaA-N-acridine (Tables 1 and 2). This indicates that there is an inverse relationship between the RRE affinity and specificity of these aminoglycoside−acridine conjugates. Consistent with this, Wong et al. have established a correlation between the number of amines on aminoglycosides with their nonspecific binding affinity for an A-site hairpin (*44*). The same relationship is apparent with the *unmodified* aminoglycosides for binding to both the RRE66 and poly r[A]−r[U], where approximately a 10-fold increase in RNA affinity is gained for each additional amine (compounds **1**−**3**, Table 1 and ref *44*). This same relationship, however, does not hold true for the acridine conjugates. For compounds **4**, **7**, and **8**, approximately a 2.5-fold increase in binding affinity is observed for each additional amine (Table 1). This may highlight a potential advantage of molecules that contain an intercalating moiety, where the relationship between charge and binding affinity is less "steep" than for compounds that solely rely upon electrostatic interactions for RNA binding.

Dimeric Aminoglycosides. Many different RNAs, including the RRE, are reported to contain multiple binding sites for neomycin B (*8*, *36*). Aminoglycoside dimers can, in principle, simultaneously occupy one or more binding sites, resulting in entropic and enthapic advantages relative to the monomeric species. The synthesis and evaluation of aminoglycoside dimers was first reported by Wang and Tor (*26*). Subsequently, it has been shown that the dimerization of neomycin B, kanamycin B, and tobramycin enhances their binding of a wide range of unrelated RNAs, including the HH16 ribozyme (*26*), $tRNA^{Phe}$ (*6*), a dimerized A-site (*45*), the *Tetrahymena ribozyme* (*46*), and the HIV-1 packaging domain (*48*). No studies, until now, have systematically examined the RNA and DNA affinity and specificity of these compounds.

Unlike the acridine conjugates, the RNA over DNA selectivity of the aminoglycoside is largely maintained upon dimerization. Both neo−neo (**9**) and neomycin B (**1**) exhibit about a 20-fold higher affinity to r(A)−r(U) as compared to CT DNA (Table 1). Most of the acridine conjugates (**6**, **7**, and **8**), on the other hand, have approximately the same or even higher affinity to duplex DNA as compared to RNA (Tables 1 and 2). The solid-phase assay gives similar results. In the presence of CT DNA, the acridine conjugates (**6**, **7**, and **8**) lose 4- through 40-fold of their Rev−RRE inhibitory activity, while the inhibitory activities of the aminoglycoside dimers (**9**, **11**, **13**) as well as RevIA (**14**) diminish very little (about 2-fold) (Table 2). The RRE specificity of the aminoglycoside dimers suffers, however, from their high affinity to many other RNAs (Tables 1 and 2).

Another group has recently published the binding of neo−neo (**9**) and tobra−tobra (**11**) to a minimized RRE construct "RREIIB-TR" (*37*). Tok et al. have reported that the dimerization of neomycin increases its RRE affinity by 17-fold (*37*). Our results indicate a 100-fold increase (Tables 1 and 2). Surprisingly, the dimerization of tobramycin was previously reported to have no effect on its RRE affinity (*37*). Our results, however, indicate that dimerization of tobramycin increases its affinity to the RRE66 by 300-fold. There are a number of potential reasons for these differences. The difficulties we have previously encountered when making serial dilutions of these compounds in pure water (i.e., significant loss of neo−neo and tobra−tobra onto pipet tips and tubes) may, in part, explain some of these discrepancies (thus decreasing the apparent activities of neo−neo and tobra−tobra). Making serial dilutions of these compounds in buffer can minimize these losses. In addition, it is possible that the aminogycoside dimers do not bind to the same sites on the RREIIB-TR as compared to the RRE66. This does not, however, seem to be a sufficient explanation, as Tok et al. have reported approximately the same affinities for RREIIB-TR binding to each of the monomeric species (tobramycin (**2**) and neomycin B (**1**)) as we have measured for the RRE66 (Table 1 and ref *37*). In addition, Tok et al. used 600 nM of RREIIB-TR to measure an RRE affinity (K_i) of 10 nM for neo−neo (**9**) (*37*). This should not, in theory, be possible, as examination of their raw data suggests that 10 nM of neo−neo somehow binds to 400 nM of the RREIIB-TR (*37*). The IC_{50} values that we report for these interactions, on the other hand, do not violate any theoretical limits for 1:1 associations, where $IC_{50} >$ 6.5 nM for RevFl displacement and $IC_{50} >$ 30 nM for

ethidium displacement experiments (see Experimental Section and Table 1).

Comparison of Aminoglycoside Dimers and Acridine Conjugates. Some trends in RRE affinity and specificity are apparent for both the aminglycoside dimers (**9**, **11**, and **13**) and the aminoglycoside−acridine conjugates (**4**, **7**, and **8**). Among all modified aminoglycosides, the kanamycin-based derivatives (**8** and **13**) exhibit the lowest RRE affinities and the best RRE specificities. Their RRE specificity ratios are similar to the ratio exhibited by the unlabeled Rev peptide (Table 2d). The neomycin-based derivatives (**4** and **9**), in contrast, exhibit the highest RRE affinities and the worst RRE specificities. The tobramycin derivatives (**7** and **11**) exhibit RRE affinities and specificities that are intermediate between those of the neomycin and the kanamycin A derivatives (Tables 1 and 2). It appears, therefore, that for both families of compounds there is an inverse relationship between their RRE affinity and specificity. A similar trend is also apparent for guanidinylated aminoglycosides (*24*), and the unmodified aminoglycosides (ref *29* and Table 2). This trend may, therefore, represent a general principle in RNA-small molecule interactions, where ligands with more charge exhibit higher RRE affinity, but lower specificity. Importantly, the ability of the kanamycin A dimer to maintain a relatively high RRE affinity *and* specificity (despite its eight amines) may indicate that charge density, not simply the total number of charges, is the key factor in maintaining both high affinity and specificity.

SUMMARY

Aminoglycoside dimers and aminolgycoside intercalator conjugates are currently the only two families of aminoglycoside derivatives that display very high affinities to RNA ($K_d \leq 10$ nM) (*13*−*17*, *23*, *34*, *37*, *43*). We have used Rev peptide and ethidium bromide displacement experiments to collect an extensive set of data that has been used to identify trends in the RNA versus DNA selectivity of these compounds, as well as their binding to the HIV-1 RRE, a pharmacologically important RNA. Interestingly, RNA over DNA selectivity (in general) is not an essential prerequisite for high RRE specificity. The neomycin-based derivatives exhibit the highest RRE affinities and maintain RNA over DNA selectivity, but they display the worst RRE specificities. Among all the "high affinity" aminoglycoside-based ligands presented here, the kanamycin A-based derivatives have the lowest RRE affinities, but exhibit the best RRE specificities. The RRE affinities and specificities of the tobramycin derivatives are intermediate between those of the neomycin and kanamycin A derivatives. This suggests that there is an *inverse* relationship between the RNA affinity and RRE specificity exhibited by aminoglycoside derivatives. This relationship may represent a general principle of small-molecule RNA binding, and it highlights the true challenge in this field: the design and synthesis of RNA ligands with *both* high affinity *and* high specificity for a predetermined RNA target. Indeed, we have demonstrated that high affinity RNA ligands are relatively easy to obtain via aminoglycoside dimerization or attachment of an intercalating agent. Few of the resulting compounds, however, exhibit a high RRE specificity.

ACKNOWLEDGMENT

We thank Dr. Sarah Kirk for helpful discussions and a preliminary synthesis of neo-N-acridine.

SUPPORTING INFORMATION AVAILABLE

Synthesis and characterization of neo-N-acridine, neo-C-acridine, tobra-N-acridine, kana-N-acridine, neo−neo, neomycin B conjugate, tobra-N-tobra, and neo-N-neo. ^{1}H NMR spectra of neo-N-neo, neo−neo, 5″-β-mercaptoethylether-neomycin B, and neomycin B. Representative data for the displacement of RevFl from the solid-phase immobilized RRE. This material is available free of charge via the Internet at http://pubs.acs.org.

REFERENCES

1. Jin, E., Katritch, V., Olson, W. K., Kharatisvili, M., Abagyan, R., and Pilch, D. S. (2000) *J. Mol. Biol. 298*, 95−110.
2. Moazed, D., and Noller, H. F. (1987) *Nature 327*, 389−394.
3. Lynch, S. R., and Puglisi, J. D. (2001) *J. Mol. Biol. 306*, 1037−1058.
4. Griffey, R. H., Hofstadler, S. A., Sannes-Lowery, K. A., Ecker, D. J., and Crooke, S. T. (1999) *Proc. Natl. Acad. Sci. U.S.A. 96*, 10129−10133.
5. Sucheck, S. J., Greenberg, W. A., Tolbert, T. J., and Wong, C.-H. (2000) *Angew. Chem., Int. Ed. 39*, 1080−1084.
6. Kirk, S. R., and Tor, Y. (1999) *Bioorg. Med. Chem. 7*, 1979−1991.
7. Walter, F., Vicens, Q., and Westhof, E. (1999) *Curr. Opin. Chem. Biol. 3*, 694−704.
8. Hendrix, M., Priestley, E. S., Joyce, G. F., and Wong, C.-H. (1997) *J. Am. Chem. Soc. 119*, 3641−3648.
9. Chen, Q., Shafer, R. H., and Kuntz, I. D. (1997) *Biochemistry 36*, 11402−11407.
10. Robinson, H., and Wang, A. H.-J. (1996) *Nucleic Acids Res. 24*, 676−682.
11. Cho, J., and Rando, R. R. (1999) *Biochemistry 38*, 8548−8554.
12. Hamasaki, K., Killian, J., Cho, J., and Rando, R. R. (1998) *Biochemistry 37*, 656−663.
13. Weizman, H., and Tor, Y in *Carbohydrate-Based Drug Discovery* (Wong, C.-H., Ed.) Wiley-VCH, in press.
14. Sucheck, S. J., and Wong, C.-H. (2000) *Curr. Opin. Chem. Biol. 4*, 678−686.
15. Griffey, R. H., and Swayze, E. E. (2002) *Expert Opin. Ther. Pat. 12*, 1367−1374.
16. Gallego, J., and Varani, G. (2001) *Acc. Chem. Res. 34*, 836−843.
17. Cheng, A. C., Calabro, V., and Frankel, A. D. (2001) *Curr. Opin. Struct. Biol. 11*, 478−484.
18. Luedtke, N. W., and Tor, Y. (2003) *Biopolymers (Nucleic Acid Sciences), 70*, 103−119.
19. Pollard, V. W., and Malim, M. H. (1998) *Annu. Rev. Microbiol. 52*, 491−532.
20. Malim, M. H., Tiley, L. S., McCarn, D. F., Rusche, J. R., Hauber, J., and Cullen, B. R. (1990) *Cell 60*, 675−683.
21. Chen, J.-H., Le, S.-Y., and Maizel, J. V. (2000) *Nucleic Acids Res. 28*, 991−999.
22. Zapp, M. L., Stern, S., and Green, M. R. (1993) *Cell 74*, 969−978.
23. Kirk, S. R., Luedtke, N. W., and Tor, Y. (2000) *J. Am. Chem. Soc. 122*, 980−981.
24. Luedtke, N. W., Baker, T. J., Goodman, M., and Tor, Y. (2000) *J. Am. Chem. Soc. 122*, 12035−12036.
25. Heaphy, S., Dingwall, C., Ernberg, I., Gait, M. J., Green, S. M., Karn, J., Lowe, A. D., Singh, M., and Skinner, M. A. (1990) *Cell 60*, 685−693.
26. Wang, H., and Tor, Y. (1997) *Bioorg. Med. Chem. Lett. 7*, 1951−1956.
27. Umezawa, H., and Kondo, S. (1975) *Methods Enzymol. 43*, 263−278.
28. Uhlenbeck, O. C., and Milligan, J. F. (1989) *Methods Enzymol. 180*, 51−62.
29. Luedtke, N. W. (2003) Ph.D. Thesis, University of California, San Diego.

30. Luedtke, N. W., and Tor, Y. (2000) *Angew. Chem., Intl. Ed. 39*, 1788−1790.
31. Bresloff, J. L., and Crothers, D. M. (1981) *Biochemistry 20*, 3547−3553.
32. Scatchard, G. (1949) *Ann. N. Y. Acad. Sci. 51*, 660−672.
33. Wang, Y., Hamasaki, K., and Rando, R. R. (1997) *Biochemistry 36*, 768−779.
34. Hamasaki, K., and Ueno, A. (2001) *Bioorg. Med. Chem. Lett. 26*, 591−594.
35. Due to differences in RNA quantification protocols (see Materials and Methods), we originally reported a K_d = 2.3 nM for the RevFl−RRE interaction, and a K_i = 1.5 nM for the neo-S-acridine-RRE affinity (*23*).
36. Lacourciere, K. A., Strivers, J. T., and Marino, J. P. (2000) *Biochemistry 39*, 5630−5641.
37. Tok, J. B., Dunn, L. J., and Des Jean, R. C. (2001) *Bioorg. Med. Chem. Lett. 11*, 1127−1131.
38. Unlike the minimized RRE constructs used by Marino (*36*), Tok (*37*), and Rando (*33*), the highest-affinity neomycin B binding site on the RRE66 appears capable of displacing RevFl (see refs 18 and 22).
39. Boger, D. L., Fink, B. E., Brunette, S. R., Tse, W. C., and Hedrick, M. P. (2001) *J. Am. Chem. Soc. 123*, 5878−5891.
40. Baguley, B. C., Denny, W. A., Atwell, G. J., and Cain, B. F. (1981) *J. Med. Chem. 24*, 170−177.
41. Wilson, W. D., Ratmeyer, L., Cegla, M. T., Spychala, J., Boykin, D., Demeunynck, M., Lhomme, J., Krishnan, G., Kennedy, D., Vinayak, R., and Zon, G. (1994) *New. J. Chem. 18*, 419−423.
42. Wilson, W. D., Ratmeyer, L., Zhao, M., Strekowski, L., and Boykin, D. (1993) *Biochemistry 32*, 4098−4104.
43. Tok, J. B−H., Cho, J. H., and Rando, R. R. (1999) *Tetrahedron 55*, 5741−5758.
44. Wong, C.-H., Hendrix, M., Priestley, E. S., and Greenberg, W. A. (1998) *Chem. Biol. 5*, 397−406.
45. Tok, J. B−H., and Huffman, G. R. (2000) *Bioorg. Med. Chem. Lett. 10*, 1593−1595.
46. Michael, K., Wang, H., and Tor, Y. (1999) *Bioorg. Med. Chem. 7*, 1361−1371.
47. Sucheck, S. J., Wong, A. L., Koeller, K. M., Boehr, D. D., Draker, K.-A., Sears, P., Wright, G. D., and Wong, C.-H. (2000) *J. Am Chem. Soc. 122*, 5230−5231.
48. Sullivan, J. M., Goodisman, J., and Dabrowiak, J. C. (2002) *Bioorg. Med. Chem. Lett. 12*, 615−618.
49. Wang H., and Tor, Y. (1997) *J. Am. Chem. Soc. 119*, 8734−8735.

BI034766Y